Characterization of CSC-GMAW Titanium-Rich Weld Overlays

Several Fe-X-Ti weld overlay systems were deposited and their microstructure, composition, and microhardness were characterized

BY J. E. RAMIREZ

ABSTRACT

Different Fe-X-Ti weld overlays were deposited using the controlled short-circuit gas metal arc welding (CSC-GMAW) process alone or in combination with the pulsed gas tungsten arc welding (GTAW-P) process. The overlays were characterized before and after postweld heat treatment (PWHT) using optical and scanning electron microscopy, electron probe microanalysis, and microhardness testing. Commercially pure nickel (CPNi), nickel-copper alloy (NiCu), nickel-chromium alloy (NiCr), vanadium, and CPCu were selected as interlayers for the Fe-X-Ti overlays. The Fe-Ni-Ti, Fe-NiCu-Ti, and Fe-NiCr-Ti systems welded with the CSC-GMAW process showed a high degree of intermixing resulting in wide X-Ti interfaces, the presence of second phases at the X-Ti interface and in the first Ti layer, and the formation of Widmanstätten- α microstructure in the first two Ti layers. Composition profiles indicate three Ti layers are required to achieve a CPTi composition in the overlay surface. The maximum hardness in the Fe-Ni-Ti, Fe-NiCu-Ti, and Fe-NiCr-Ti overlays were 607, 568, and 554 HV_{0.5}, respectively. On the other hand, the Fe-V-Ti and Fe-Cu-Ti overlays presented a lower degree of intermixing resulting in narrow X-Ti interfaces, presence of second phases only at the interface, and Ti weld deposits with microstructures similar to commercially pure α -Ti. Depending on the welding process, one to three Ti layers are needed in the Fe-Cu-Ti overlay for Ti-clad steel applications. The maximum hardness in this overlay ranged from 300 to 350 $HV_{0.5}$ and dropped to around 200 $HV_{0.5}$ after PWHT. The primary second phases identified in the Ti-rich weld overlays included Ni₃Ti, NiTi, NiTi₂, CuNiTi, CuTi₂, Cr₂Ti, CuTi₂, Cu₃Ti, and β -Ti.

KEYWORDS

- Ti-Clad Steels Surfacing Cladding Welding Metallurgy Overlays
- Gas Metal Arc Welding (GMAW) Gas Tungsten Arc Welding (GTAW)

Introduction

Titanium (Ti) clad steels are widely

used for large pressure vessels and other equipment in different industries to take advantage of the corrosion resistance of Ti, but at a lower cost than solid Ti construction. Ti-clad steels are produced by roll bonding (usually with an interlayer), direct explosive bonding (usually without an interlayer) (Ref. 1), or by a combination of explosive bonding and roll bonding (Ref. 2). Interlayers are used to improve the bond strength of the clad steel or to overcome metal plasticity compatibility restrictions encountered in roll bonding. Industrial-grade pure iron (Fe); ultralow-carbon steel; and niobium (Nb), tantalum (Ta), copper (Cu), and nickel (Ni) alloys have been used as interlayers in the cladding process (Refs. 3-6). Ti is also used in lightweight applications due to its high strength-to-weight ratio. This has led to the use of Ti and its alloys in a wide range of applications in aerospace, marine/submarine, automobiles, and as a bio-implant material.

Sometimes there is the need to repair corrosion-resistant Ti-clad steels during production or during service. Additionally, poor wear/erosion resistance is a serious drawback for more universal applications of titanium or titanium alloys. Corrosion and wear are essentially surface-related phenomena. Therefore, suitable modification of surface composition and/or microstructure is a logical and economical approach to provide corrosion or wear resistance of structural elements. Therefore, development of Tirich overlays to weld corrosionresistant Ti-clad steels or to provide erosion/wear resistance to lightweight Ti structures is needed. However, Ti

J. E. RAMIREZ (jose.ramirez@dnvgl.com) was a principal engineer with EWI, Columbus, Ohio, at the time this work was completed. Currently, he is a principal engineer at DNV.GL, Columbus, Ohio.

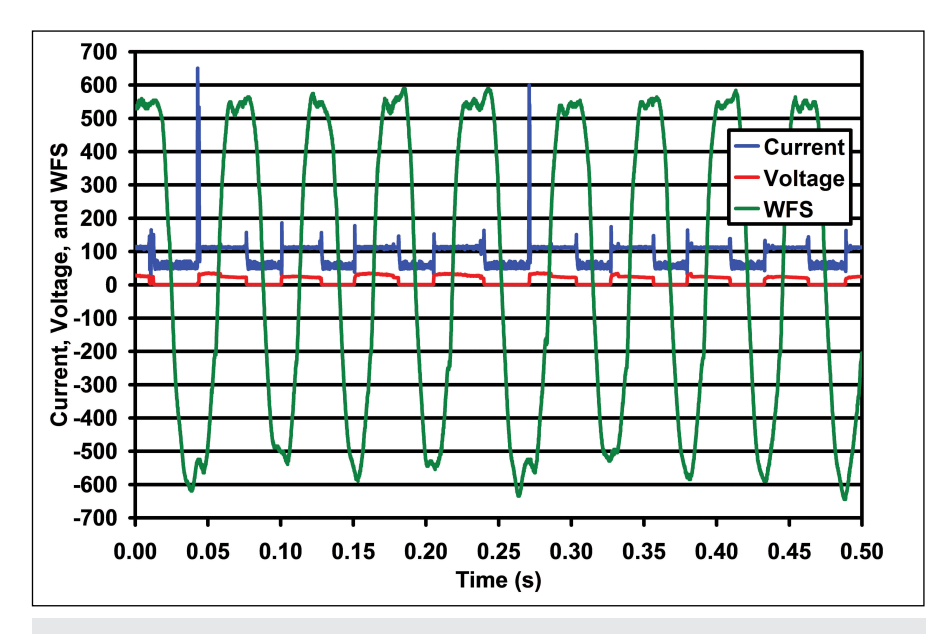


Fig. 1 — Schematic plot of current, voltage, and WFS waveform of a typical CSC-GMAW weld over $0.5\ s.$

has not been successfully fusion welded directly to steel or other common alloy systems because Ti has limited solubility for them. Brittle intermetallic compounds and carbides form when the solubility limit is exceeded, as in fusion welding (Refs. 7, 8). Cracks often form in these brittle phases due to the thermal stresses induced during cooling of the welded joint. In order to identify potential Tirich overlay systems for welding or repairing Ti-clad steel plates or to provide wear/erosion resistance for lightweight Ti structures, different Fe-X-Ti weld overlay systems were deposited and characterized, with or without postweld heat treatment (PWHT), in this experimental work.

Experimental Procedures

Selection of Interlayer Materi-

als: An extensive literature search was conducted to identify the different technical approaches that have been evaluated to date to avoid or control the embrittlement normally found in steel-to-Ti joints. The metallurgical characteristics of different potential interlayer materials as they relate to the compatibility with the Ti-Fe system were reviewed. Five interlayer materials were selected for use in the Fe-X-Ti weld overlays.

Efforts involving combinations of joining processes and interlayer mate-

rials between the Ti and steel to control or completely avoid the intermixing of steel and Ti have resulted in limited success. These efforts include resistance welding with vanadium (V), molybdenum (Mo), aluminum (Al), or silver (Ag) interlayers (Ref. 10); arc welding after the steel has been metallized or plasma sprayed with a layer of Mo, tungsten (W), tantalum (Ta), or refractory carbides (Refs. 11-13); diffusion bonding with a Ni interlayer or controlling the carbon level in the steel plate (Refs. 14, 15); friction welding with and without a frictionweldable interlayer (Refs. 16, 17); instantaneous liquid phase bonding (Ref. 18); and electron beam welding using Ag insert metal (Ref. 19). Additionally, data on dissimilar-metal joints involving a combination of Ti, steel, and other alloys and their associated mechanical properties are limited. Finally, despite previous efforts, there is not a clear understanding of the relative embrittlement effect of carbides and the different intermetallic compounds that may form when Ti is joined to Fe, Ni, or Cu.

Data available on theory of alloying, binary and ternary phase diagrams, and the quasi-equilibrium behavior of these alloy systems during solid-state bonding or roll bonding do not include the effect of nonequilibrium conditions induced during weld thermal cycles. However, they provided insight and were used as general guidelines to select the potential interlayer materials for the Ti-rich weld overlay systems, as described as follows

V Interlayer: The Fe-Ti phase diagram shows limited mutual solubility and the presence of intermetallic compounds (Fe₂Ti and FeTi). Additionally, carbon in the steel may react with Ti to form brittle carbides (TiC). Alloying is an important means of reducing the negative effect of brittle intermetallic compound formation on weldability. The stabilization of thermo dynamically ideal solid solutions could reduce the tendency for intermetallics to form. The equilibrium phases Fe₂Ti and FeTi form at specific electron/atom (e/a) ratios. Any ternary alloying element affecting the e/a ratio likely affects the stability of these intermetallic phases.

Based on the theory of alloying, it has been indicated that size difference between solute and solvent atoms is important in determining the stability of solid solutions (Ref. 20). If the atomic radii of the solute and the solvent differ by more than 15%, extensive solubility is unlikely. If the solute and the solvent radii are similar, a large mutual solubility is predicted unless solute and solvent are transition metals. Additionally, an electronegativity factor was introduced later on to complement the size factor rule (Ref. 21). A large electronegativity difference can provide a large driving force for the formation of compounds. Conversely, a small difference of electronegativity between solute and solvent atoms (less than 0.4 units) should promote a large solid solubility. These criteria have shown to be valid for a large number of systems but the predictive accuracy is poor in systems with solvents that are transition metals. However, this is still considered to be an effective tool to predict mutual solubility of alloying elements. In a graphical representation or Darken-Gurry type map for Fe and Ti (Ref. 22), each of these elements represents the center of an ellipse with principal radii corresponding to 15% of atomic radius and 0.4 electronegativity units. As a result, V and other elements (including manganese and chromium) located inside both these ellipses are, according to these criteria, potential

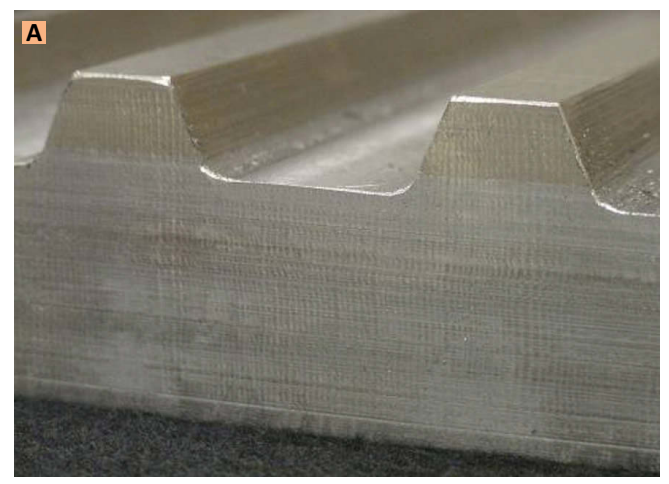








Fig. 2 — A, B — General view of Ti-clad steel wide groove joint design; C — Ti-rich weld overlays deposited with the CSC-GMAW process; D — weld overlays deposited with a combination of the CSC-GMAW and GTAW-P processes.

candidates for joining Fe to Ti.

Few reliable theories have been developed to determine the solid solubility of alloys in which both solute and solvent are transition metals; however, an empirical diagram has been proposed that maps elements as a function of their electron density and chemical potential (Fermi energy) (Refs. 22-24). It was discovered that the absolute value of the ratio of these two quantities characterized well the sign of heat of mixing, and could be used as a general rule for alloying. This type of diagram for the transition metals and selected nontransition elements shows that V lies almost exactly between Ti and Fe (Ref. 22). The addition of V causes the Fermi energy of Fe to decrease at a rate approximately equal to that of the increase in Fermi energy of Ti. Thus, the addition of V causes the lattice mismatch between BCC-Fe and β-Ti to decrease.

Because the primary selection of alloying elements for the weld overlays is restricted to those potentially forming simultaneously continuous series of solid solution with Fe and Ti, the

primary choice is V. Other elements that may be considered as a secondary choice and that are part of commercially available welding wires include Ni and chromium (Cr).

Ni and Ni-Cu Interlayers: There are additional reasons to use Ni as an interlayer material. The addition of Ni suppresses the formation of Ti-Fe intermetallic compounds. Studies of properties of diffusion joints between Ti and mild steels also indicate that using a Ni interlayer results in the formation of intermetallic compounds rich in Ti and Ni but with better properties than those where Ti was joined directly to the steel (Ref. 14). Furthermore, Ni and Fe form continuous series of solid solution at high temperature. Finally, it is difficult to form carbides in Ni alloys. Experimental results have shown that the coexistence of TiFe and TiFe₂ with TiC will have more detrimental effects on the properties of the joint than if only one compound is formed (Ref. 15).

Ni-Cr Interlayer: Studies of hot rolling Ti-clad steels between 850° and 1010°C with a Ni-Cr interlayer showed that when Cr content is below 32.5 wt-

%, a brittle Ti(Ni, Cr)₃ is formed at the boundary between the cladding and the insert material, which decreases the cladding strength (Ref. 6). When the Cr content exceeds 40 wt-%, a brittle δ -phase is formed at the boundary of the steel base material and the insert material. Chromium content between 32.5 and 35.0 wt-% is preferred. Additionally, when Ni content is below 55.0 wt-%, a brittle TiCr₂ is formed at the boundary of the cladding material. When the Ni content exceeds 65%, the brittle Ti(Ni, Cr)3 is formed as in the case where the Cr content is below 32.5 wt-%. Both of these situations decrease the strength of the cladding.

Since nonequilibrium welding conditions may limit the formation of the detrimental intermetallic compounds described previously, a commercially available Ni-Cr based filler metal (55–44 wt-%) with a chemical composition close to the identified optimum concentration levels was selected as potential interlayer for the Ti-rich weld overlays.

Cu Interlayer: Rapid conduction of heat from the molten weld pool by a base metal with high thermal conduc-

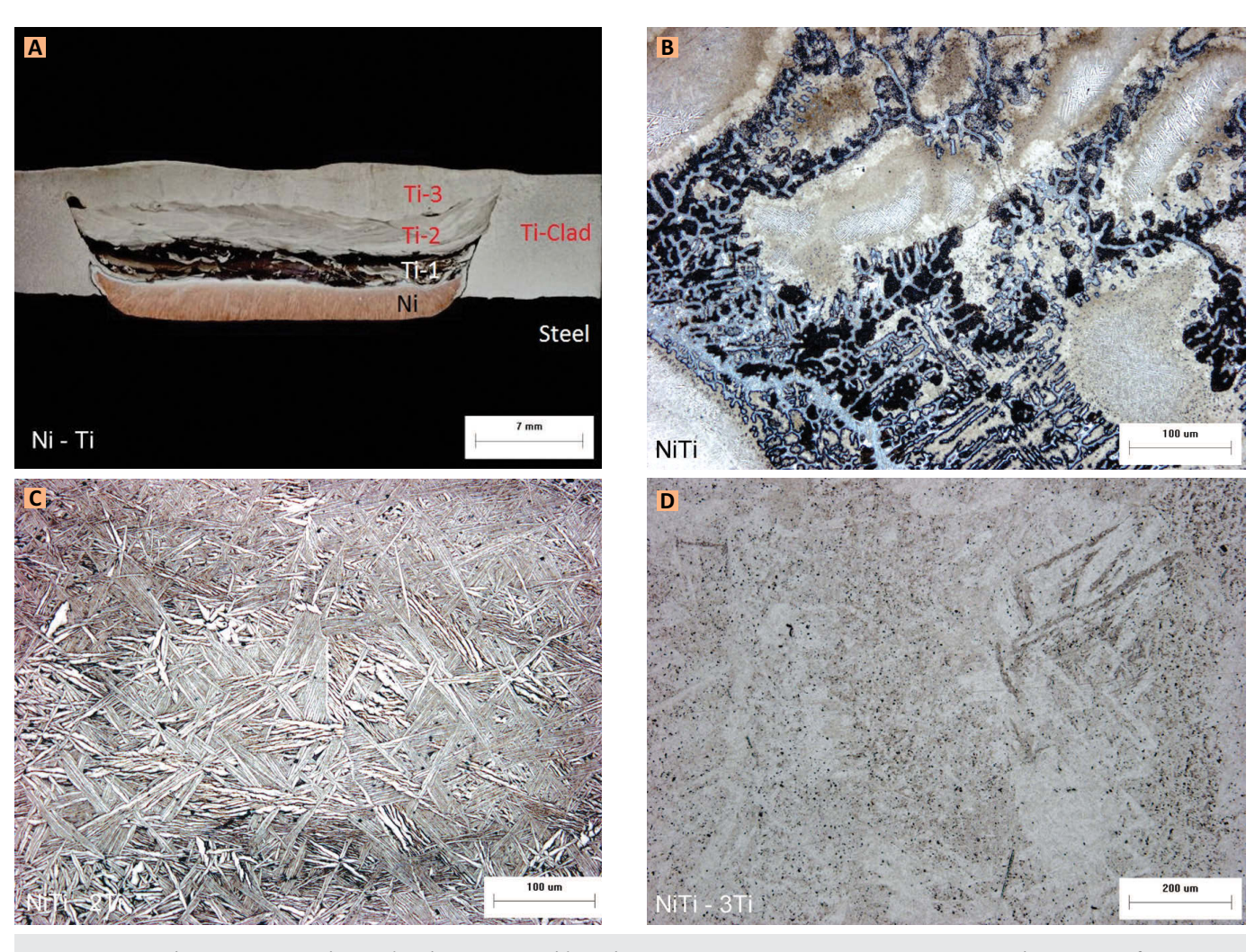


Fig. 3 — General microstructure observed in the Fe-Ni-Ti weld overlay system. A — Macro, B — Microstructure at the Ni-Ti interface. C — Microstructure of the 2nd Ti layer, D — Microstructure of the 3rd Ti layer.

tivity affects the energy available to locally melt the base metal. Reducing the amount of melting of the base metal reduces the amount of dilution of the deposited weld metal. Cu has a thermal conductivity that is about eight times higher than steel and a high preheat is normally required to melt it into the weld joint. Therefore, the use of a Cu interlayer may result in an undiluted Ti weld deposit, which is necessary to maintain the corrosion resistance required for the different applications of Ti-clad steels.

Additionally, the high ductility of copper may accommodate the large strain induced in the weld overlays during cooling. Therefore, commercially pure (CP) Cu was also selected as a potential interlayer for the weld overlays.

In summary, based on a comprehensive literature review, potential

interlayer materials for the Ti-rich overlays were identified based on their metallurgical characteristics and compatibility with the Ti-Fe system. The selected interlayer materials included:

- Vanadium (V): This interlayer material was selected since it is potentially compatible with, and has a higher melting temperature than, both Ti and Fe.
- Copper (Cu): This interlayer material
 was selected because it has a lower
 melting temperature and a higher
 thermal conductivity than both Ti
 and steel. Therefore, it is expected to
 minimize the amount of dilution and
 interaction between them.
- Nickel (Ni) based interlayers: These interlayer materials were selected to try to control the type of phases formed at the interface and the resulting degree of embrittlement of the joint.

Welding Conditions: Different joining processes were considered for the deposition of the different weld overlay systems (Ref. 9). The selection criteria included that the material overlay-joining process combination should be easily deployed in the field, require a low equipment investment, and use commercially available consumables. Therefore, arc welding processes were considered the primary processes of choice. The controlled short-circuit gas metal arc welding (CSC-GMAW) process offers significantly reduced heat input and dilution when compared to other arc welding processes. Therefore, the CSC-GMAW process was chosen to deposit most of the selected interlayer materials and Ti layers. The CSC-GMAW process is an advanced version of the short-circuiting GMAW process, which uses a reciprocating wire feed to







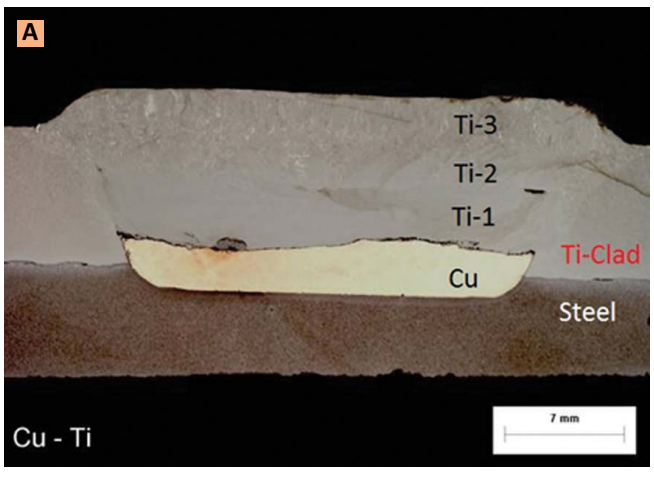
Fig. 4 — General microstructure observed in the Fe-V-Ti weld overlay system. A — Macro, B — Microsturcture at the V-Fe interface, C — Microstructure at the Ti-V interface.

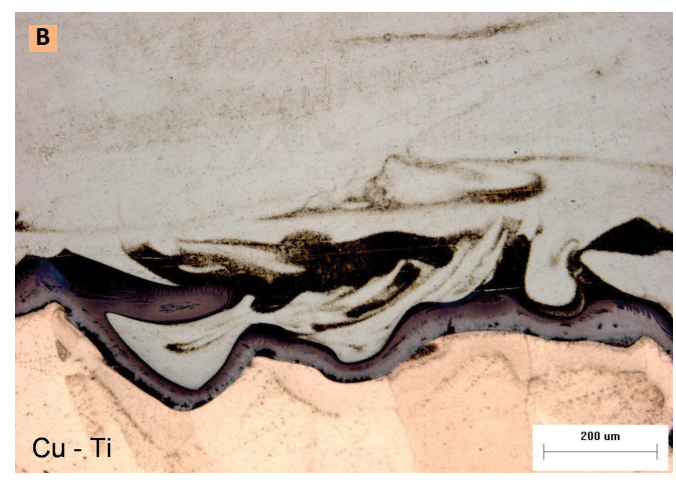
promote consistent droplet transfer at low currents (Refs. 25–29).

Welding parameters of the CSC-GMAW process include up-wire feed speed (Up WFS) (m/min), down-WFS (m/min), arc length (mm), arc current sequence, and short circuit current sequence. Each current sequence has three levels to set (start, pulse, and end). These three current levels are used to control the bead shape and size. The start and pulse levels have a time associated with them. For the end current level,

Table 1 — Welding Conditions for Deposition of Different Layers of Materials in the Weld Overlays Using the CSC-GMAW Process

			Arc Current Sequence			Short Circuit Current Sequence					
Weld Layer	Shielding Gas	Start Current (A)	Start Current Time (ms)		Pulse Current ïme (ms)	End Current (A)	Start Current (A)	Start Current Time (ms)	Pulse Current (A)	Pulse Current Time (ms)	End Current (A)
Ni on Steel	100% He	100	NA	100	NA	100	50	NA	50	NA	50
Ti on Ni	100% He	80	5	60	5	40	40	2.5	60	NA	60
NiCu on Steel	100% He	100	NA	100	NA	100	50	NA	50	NA	50
Ti on NiCu	100% He	80	5	60	5	40	40	2.5	60	NA	60
NiCr on Steel	50% Ar/50% He	100	NA	100	NA	100	50	NA	50	NA	50
Ti on NiCr	100% He	80	5	60	5	40	40	2.5	60	NA	60
CPCu on Steel	100% He	130	NA	130	NA	130	50	NA	50	NA	50
CPCu on Steel	100% He	150	NA	150	NA	150	50	NA	50	NA	50
Ti on CpCu	100% He	120	5	100	5	80	40	2.5	60	NA	60
Ti on Ti	100% He	80	5	60	5	40	40	2.5	60	NA	60
			Wire Feed Speed			Weaving Parameters					
			Up WFS (m/min)	Down WFS (m/min)	Arc Lengt (mm)		tion Speed i./min)	Dwell Time (s)			ed
			10	15	0.0		17.4	0.2	0.78	65	.1
			8	10	1.0		28.4	0.3	0.90	27	
			10	15	0.0		22.3	0.2	0.80	65	.1
			8	10	0.5		28.4	0.3	0.93	27	.9
			15	15	0.0		17.4	0.2	0.83	74	.4
			8	10	0.5		28.4	0.3	0.88	27	.9
			15	15	0.0		34.5	0.3	0.70	26	.0
			10	10	0.0		46.8	0.3	0.65	26	.0
			8	10	0.0		28.4	0.3	0.83	29	.7
			8	10	0.5		28.4	0.3	0.93	27	.9





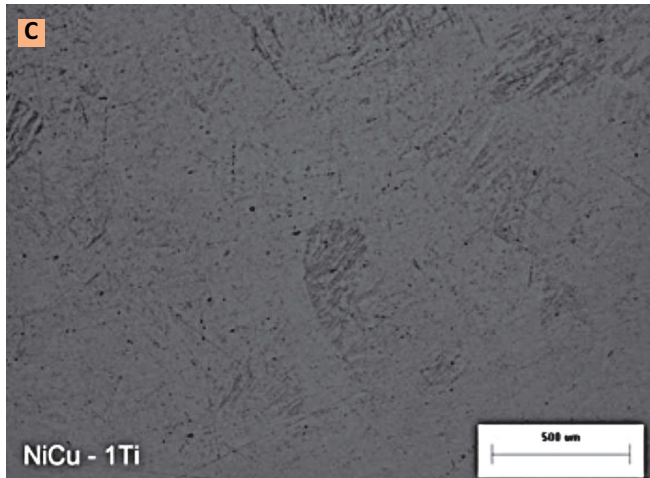




Fig. 5 — General microstructure observed in the Fe-Cu-Ti overlay system: A — Macro; B — Microstructure at the Cu-Ti interface, C — Microstructure of the 1^{st} Ti layer, D — Microstructure of the 3^{rd} Ti layer.

 ${\it Table 2-General Characteristics of the Welding Consumables Used to Deposit the Ti-Rich Weld Overlays } \\$

Weld Overlay System ^(a)	Interlayer Material	Filler Metal Designation	Wire Size (in.)	Welding Process
1. Ni-Ti	Nickel	ERNi-1	0.062	CSC-GMAW
2. NiCu-Ti	Nickel-copper	ERNiCu-7	0.062	CSC-GMAW
3. NiCr-Ti	Nickel-chromium	ERNiCr-4	0.062	CSC-GMAW
4. V-Ti	Vanadium	_	0.062/0.045	P-GTAW
5. Cu-Ti	Copper	ERCu	0.062	CSC-GMAW
6. Ti	Titanium fill passes	ERTi-1	0.062/0.035	CSC-GMAW P-GTAW

(a) The designation of the weld overlay system indicates the sequence of deposition of the interlayer material and Ti in the joint.

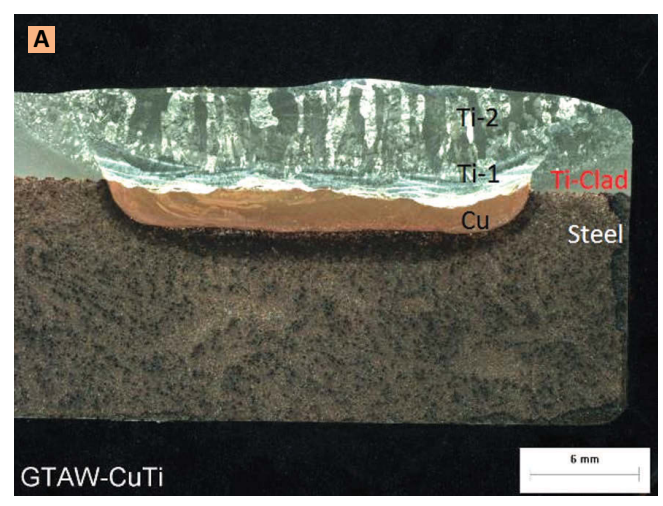
the current is maintained until the next sequence is initiated. During the arc phase, the end of the electrode is melted and a droplet is formed. At the same time, the electrode is feeding forward toward the weld pool. The forward WFS is set higher than the burn-off rate so that the arc will short out. Upon shorting, the droplet at the end of the electrode is pulled into the

weld pool by the liquid pool's surface tension. The control system senses the voltage drop and prevents the current from spiking severely. A current sequence is implemented to allow resistive heating. The heat allows for a smooth arc ignition. At the same time, the wire feeders reverse direction so that the electrode is being pulled away from the weld pool. This makes the

short circuit break mechanically. This differs from any other short circuiting process, which relies on the electrode exploding to reestablish the arc. Some of the Ti-rich weld overlays were deposited with a combination of CSC-GMAW and pulsed gas tungsten arc welding (GTAW-P) processes.

Figure 1 shows a schematic plot of the current, voltage, and wire feed speed (WFS) of a typical CSC-GMAW weld over 0.5 s. Table 1 lists the CSC-GMAW welding parameters used for depositing each interlayer material and the subsequent Ti layers in the weld overlays.

The deposition of the different interlayer materials and corresponding Ti layers was done in 150×200 -mm (6 \times 8-in.) explosion Ti-clad steel samples. The explosion-clad metals consisted of SA-516-70 carbon steel with a nominal thickness of 27.5 to 38.0 mm (1.1 to 1.5 in.) and SB-265-1 Ti clad with a nominal





thickness between 4.8 and 8.0 mm (0.188 and 0.313 in.). The samples have a wide groove prepared by the stripback method. The joint design of the wide-groove included a root that was between 19.0 and 25.0 mm (0.75 and 1.0 in.) wide and a 22-deg bevel angle. Additionally, the groove was machined to a depth of about 2.50 mm (0.10 in.) into the steel substrate, as shown in Fig. 2A, B.

The general description of the welding consumables used for the different Ti-rich weld overlay systems is included in Table 2. The designation of the weld overlay system indicates the sequence of deposition of the interlayer material and Ti in the weld overlay. For all the weld overlays deposited with the CSC-GMAW process, a 1.6-mm- (0.062-in.-) diameter electrode was used.

Figure 2C, D shows a general view of some of the weld overlay samples. The specimen in Fig. 2C shows a stepwise configuration at the ends. The three levels of the stepwise configura-



Fig. 6 — General microstructure observed in the Fe-Cu-Ti weld overlay deposited with a combination of CSC-GMAW and GTAW-P processes. A — Macro, B — Microstructure at the Cu-Ti interface, C — Microstructure of the 2^{nd} Ti layer.

tion from the end toward the center of the sample correspond to the surface of the weld deposit of the interlayer material, the surface of the first Ti deposit layer, and the surface of two additional layers of Ti. This

arrangement allowed the characterization of deposits of the interlayer material in the as-welded condition and an evaluation of the effects of thermal cycles induced during the deposition of one and three layers of Ti on the properties of the interlayer materials and the weld overlay as a whole. These welded joints were subjected to radiographic examination to evaluate the soundness of the joints and to determine the location of different specimens required for the characterization.

Postweld Heat Treatment: The PWHT of the Ti-rich overlays was conducted following the guidelines of Section VIII of the ASME, *Boiler and Pressure Vessel Code*, for carbon steel welded constructions. The holding temperature was between 1125° and 1150°F, and the holding time ranged from 1 h, 15 min to 1 h, 52 min depending on the thickness of the full-size joint. Heating rates above 800°F were controlled to be equal or less

than 400°F/h/in. Cooling rates above 800°F were equal or less than 500°F/h/in.

Microstructural Evaluation: The characterization of the Ti-rich weld overlays was conducted in the aswelded and postweld heat treated conditions. Transverse and longitudinal specimens were cut from the Ti-rich weld overlay samples for microstructural evaluation, which was conducted using optical and scanning electron microscopy (SEM), electron probe microanalysis (EPMA), and microhardness testing.

The samples were initially ground and polished using 80 to 2400 grit SiC abrasive paper. Final polishing of the samples for light microscopy and SEM was done with a 0.05-µm colloidal silica suspension. The general microstructures of the weld overlay deposits were revealed for analysis in the light microscope by using a specific combination of etchants. For the Ni-Ti, NiCu-Ti, NiCr-Ti, and Cu-Ti interlayer systems a two-step combination of Kroll (100 mL $H_2O + 2-6$ mL nitric acid 65% + 1–3 mL hydrofluoric acid 40%) and ferric chloride (3 g $Fe_3Cl + 5$ mL HCl + 100 mL H₂O) etchants were applied by immersion or swabbing. For the V-Ti interlayer system, an electrolytic etching (75 mL methanol 99.8% + 10 mL sulfuric acid 95-97% + 25 mL hydrochloric acid 32%) was used. The samples prepared for evaluation in the SEM were in the as-

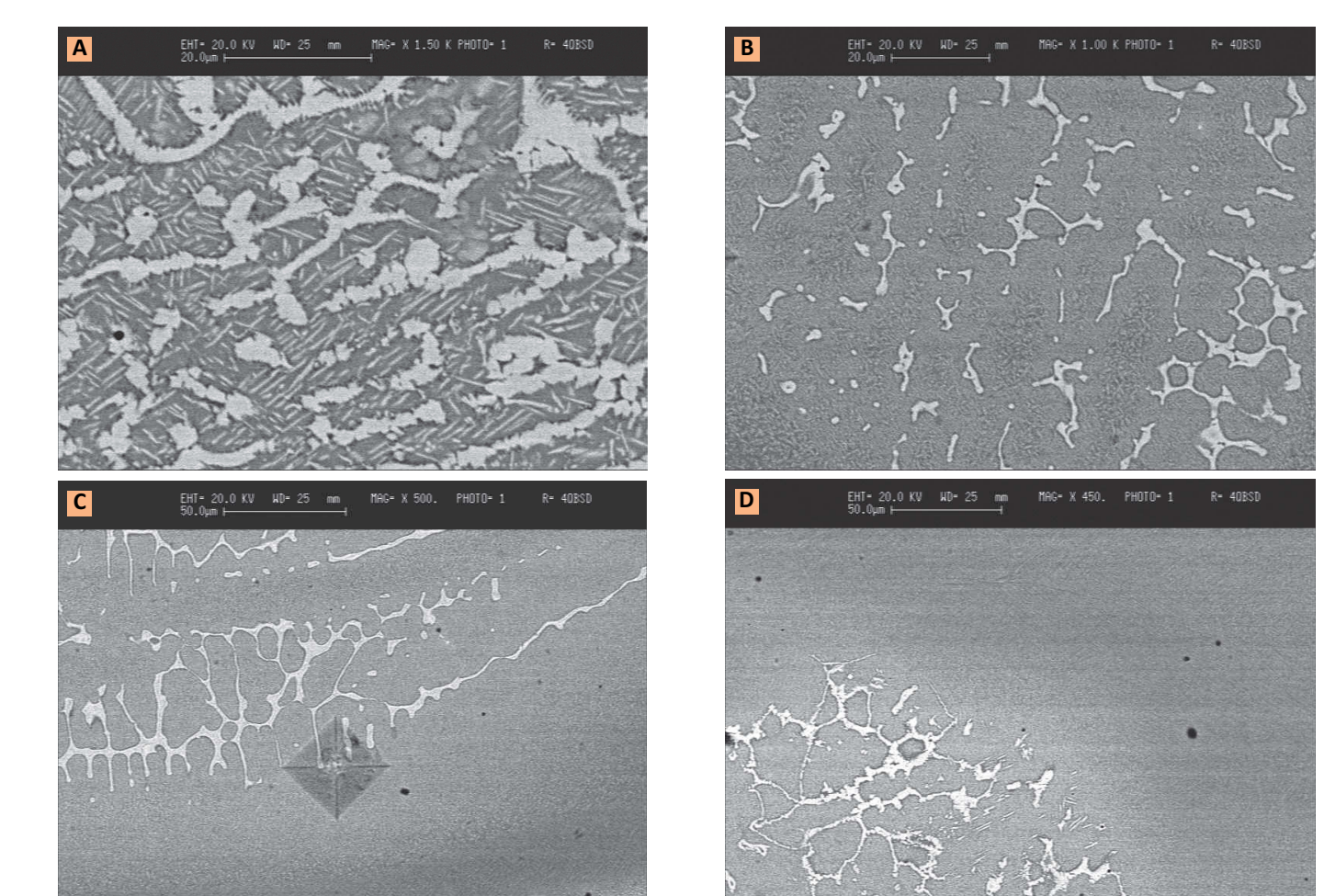


Fig. 7 — Backscattered electron images showing fraction and distribution of phases (light regions are NiCr-rich phases and dark regions are Ti-rich phases) observed in the NiCr-Ti interface (A) and in the first, second, and third Ti layers (B—D) of the weld overlay.

polished (unetched) condition.

The different phases present in each Fe-X-Ti weld overlay system were identified using the SEM in the backscattered electron mode. The chemical composition of each phase was determined using the EPMA. The combined SEMbackscattered mode and EPMA analysis were run at zones located at increasing distances from the steel-interlayer interface. The chemical composition profile of major alloying elements in the through-thickness direction of the different Ti-rich weld overlays was determined as well.

Microhardness profiles were determined in the through-thickness direction of the deposited weld overlays starting from the steel substrate toward the surface of the last layer of Ti weld deposit. The microhardness profiles of the weld overlays were determined in deposits with one and three Ti layers, respectively, and in the

as-welded and PWHT conditions. The hardness readings were determined using a hardness Vickers scale with a load of 500 g (HV_{0.5}).

Results and Discussions

Light Microscopy Evaluation:

Figures 3–6 show examples of the microstructures observed in the different overlay systems. For sake of clarity, the base materials (steel and Ti-clad) and the different deposited weld layers (interlayer material, first Ti layer, second Ti layer, and third Ti layer) are labeled in the figures showing a macrosection of the overlays (Figs. 3A, 4A, 5A, and 6A).

A high degree of intermixing between the interlayer material and Ti was observed in the Ni-Ti, NiCu-Ti, and NiCr-Ti overlays. As a result, each layer of the deposited weld overlay etched distinctly, as shown in Fig. 3A. These systems present a continuous, wide, and poorly defined interface between the interlayer material and the first Ti layer, as shown in Fig. 3B. Additionally, second phases were observed at the interlayer-Ti interface and in the first Ti layer. In the NiCr-Ti system, the presence of second phases was observed even in the third Ti layer. The formation of second phases may have resulted from dilution of Ni, Cu, or Cr in the Ti weld deposit above the solubility limit of the corresponding alloying system.

The dilution of Ni, Cu, or Cr from the interlayer material in the second layer of Ti weld metal induced the formation of acicular- or Widmanstätten- α microstructure (Fig. 3C) that is characteristic in α - β Ti alloys. Ni, Cu, and Cr are β stabilizers in Ti alloys. As expected, the stabilization of β phase decreases with a decrease in the alloying

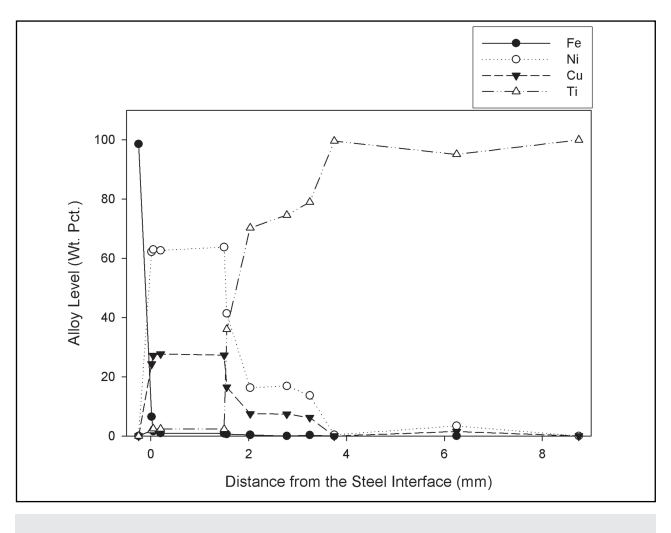


Fig. 8 — Concentration profile of Fe, Ni, Cu, and Ti in a Fe-NiCu-Ti weld overlay.

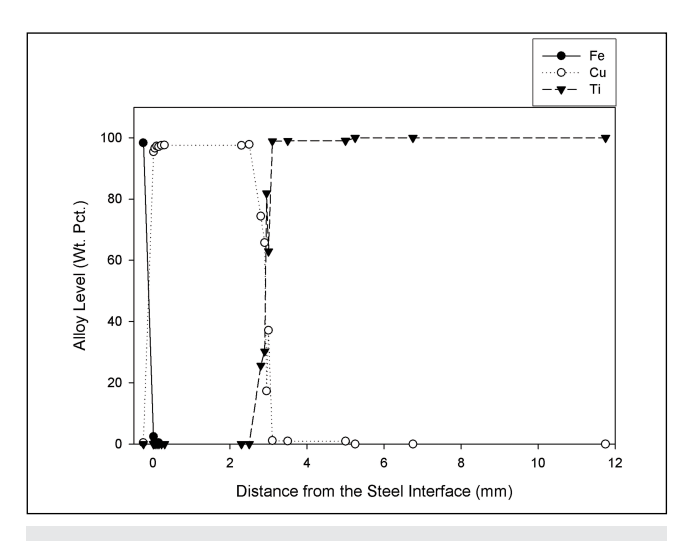


Fig. 9 — Concentration profile of Fe, Cu, and Ti in a Fe-Cu-Ti weld overlay.

content in the weld deposit. As a result, the microstructure observed in the third Ti layer, Fig. 3D, resembles more the microstructure characteristic of commercially pure or α -Ti alloys.

Conversely, the V-Ti and Cu-Ti overlay systems welded with the GTAW and the CSC-GMAW, respectively, presented a lower degree of intermixing between the interlayer material and Ti, as shown in Figs. 4A and 5A. As a result, a narrow and well-defined interface ranging in thickness from 50 to 250 μm between the Cu interlayer and Ti was observed, as shown in Fig. 5B. In these overlays, the presence of second phases was mainly limited to the Fe-V interface or the Cu-Ti interface, as shown in Figs. 4B

and 5B. The interface between V and Ti was free from formation of second phases as shown in Fig. 4C. This can be explained using the Ti-V binary phase diagram, which indicates complete solid solubility between those two elements.

Due to the low dilution of alloying elements from the interlayer material in the Ti weld deposits in these overlays, the microstructure of the Ti weld deposit, including the first layer, corresponds to those normally found in commercially pure α -Ti alloys as shown in Fig. 5C, D.

In the Cu-Ti weld overlay deposited with a combination of CSC-GMAW and the GTAW-P processes, a high degree of intermixing was observed. As a result,

each weld deposit layer etched distinctly, as shown in Fig. 6A. Additionally, the Cu-Ti interface became wider than in those made with only the CSC-GMAW process. The thickness of the interface was about 1 mm as shown in Fig. 6B. Finally, the higher level of Cu concentration in the Ti weld deposit resulted in a microstructure that is similar to those of α - β Ti weld metal alloys as shown in Fig. 6C. Cu stabilizes β-phase in Ti alloys. The thicker interface between Cu and Ti and the higher level of Cu dilution in the Ti weld deposit may be explained by the higher heat input and higher level of stirring of the weld pool induced by the GTAW-P process as compared to that of the CSC-

Table 3 — General Microstructural Characteristics Observed in the Ti-Rich Overlay Systems

	Weld Overlay System				
Characteristics	Fe-Ni-Ti Fe-NiCu-Ti Fe-NiCr-Ti	Fe-V-Ti Fe-Cu-Ti	Fe-Cu-Ti (CSC-GMAW + GTAW-P Processes)		
Degree of Intermixing Interlayer-Ti Interface	HighContinuousWidePresence of 2nd phases	 Low Continuous Narrow (<250 µm) Presence of 2nd phases (Fe-Cu-Ti system) 	 High Continuous Wide (±1.0-mm) Presence of 2nd phases 		
1st Ti Layer	 Presence of 2nd phases Acicular (α + β) Ti alloy microstructure 	 α-Ti alloy microstructure 	 Acicular (α+β) Ti alloy microstructure 		
2nd Ti Layer	 Second phases (Fe-NiCr-Ti system) Acicular (α + β) Ti alloy microstructure 	 α-Ti alloy microstructure 	 Acicular (α+β) Ti alloy microstructure 		
3rd Ti Layer	 Second phases (Fe-NiCr-Ti system) α-Ti alloy microstructure 	α-Ti alloy microstructure	• NA		

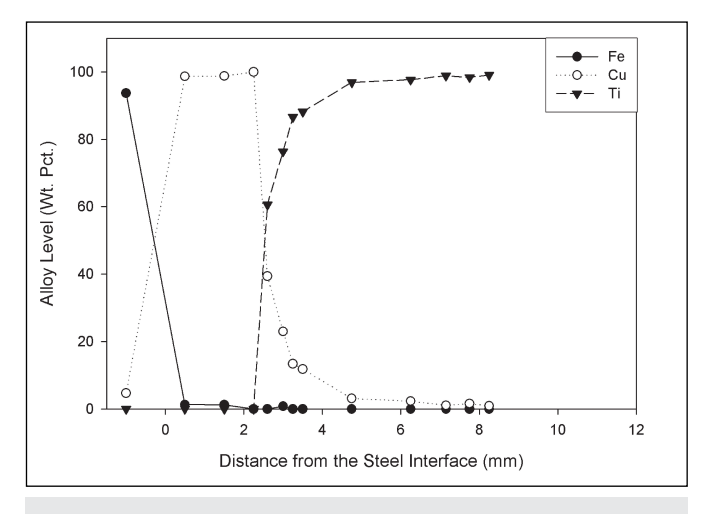


Fig. 10 — Concentration profile of Fe, Cu, and Ti in a Fe-Cu-Ti weld overlay deposited with a combination of CSC-GMAW and GTAW-P processes.

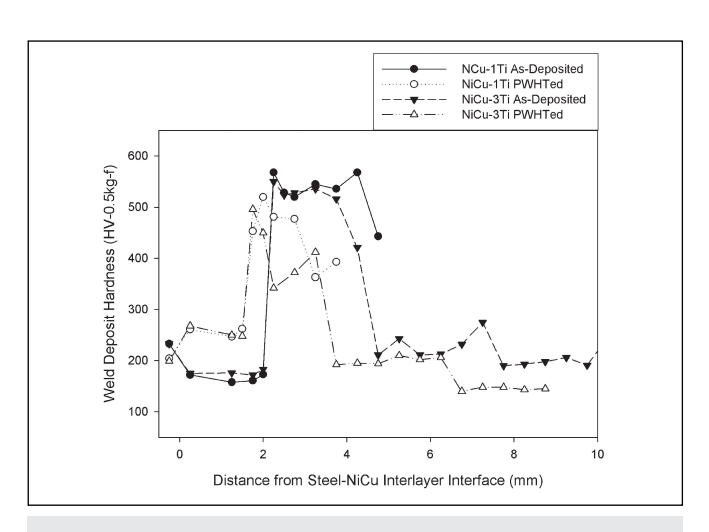


Fig. 11 — Microhardness profile of NiCu-Ti weld overlays with one and three Ti layers (1Ti, 3Ti), in the as-welded and PWHT conditions (CSC-GMAW process).

Table 4 — Chemical Composition and Designation of Potential Phases Observed in Ti-Rich Weld Overlays

	Ni	Chemical Cu	Chemical Composition, wt-% (at%) Cu Cr Ti				
Phase			Ni-Ti Interlayer Systen	n			
1	72.8 (68.6)	_	_	27.1 (31.4)	Ni ₃ Ti		
2	59.2 (54.0)	_	_	39.7 (44.3)	NĬTI		
3	34.7 (30.2)	_	_	64.4 (68.9)	NiTi ₂		
4	27.0 (23.0)	_	_	72.7 (76.3)	NiTi ₂		
5	10.7 (8.9)	_	_	89.1 (90.7)	β-Ti¯		
		١	NiCu-Ti Interlayer Syste	em			
1	42.7 (38.7)	23.3 (19.6)		30.6 (34.0)	CuNiTi / Ni ₃ Ti		
2	33.2 (28.5)	14.1 (11.2)	_	47.7 (50.3)	NiTi		
3	26.5 (23.1)	7.1 (5.7)	_	64.6 (69.1)	NiTi ₂ + CuTi ₂		
4	9.5 (7.7)	4.2 (3.2)	_	86.0 (88.4)	-β-Ti		
5	7.4 (6.2)	7.2 (5.6)	_	84.5 (87.0)	β-Ті		
	NiCr-Ti Interlayer System						
1	26.5 (22.8)	_	4.2 (4.1)	69.3 (73.1)	NiTi ₂		
2	9.1 (7.6)	_	9.6 (9.0)	81.3 (83.4)	NiTi ₂ + Čr ₂ Ti		
3	25.7 (22.2)	_	10.1 (9.9)	64.2 (68.0)	NiTi ₂		
4	9.5 (8.0)	_	15.4 (14.7)	75.0 (77.3)	NiTi ₂ + Čr ₂ Ti		
Cu-Ti Interlayer System							
1	_	74.4 (68.6)	_ ` `	25.6 (31.4)	CuTi ₂		
2	_	65.8 (55.8)	_	30.2 (34.0)	Cu ₃ Tī		
3	_	37.1 (30.8)	_	62.9 (69.2)	CuTi ₂		
4	_	17.3 (13.7)	_	81.9 (86.0)	β-ті		

GMAW process.

Table 3 presents a summary of the general microstructural characteristics observed in the different weld overlays by using light microscopy.

Electron Microscopy Evaluation:

Figure 7 presents, as an example, backscattered electron images illustrating the change in area fraction and distribution of different phases present in the NiCr-Ti overlay. As expected, the area fraction or quantity of phases rich in interlayer alloying elements (light phases) decreases from

the interface toward the surface of the Ti-rich weld overlay. Most of the overlays presented a dendritic solidification mode.

Chemical composition data obtained from EPMA analysis and phase diagrams related to the weld overlay systems were used to identify the potential primary phases present at the interface and in the first Ti layer. The potential phases present in each one of the weld overlay systems are listed in Table 4. Additional work, including transmission electron

microscopy or X-ray diffraction, would be required to confirm the structure and identification of these phases.

Chemical Composition Profiles:

Composition profiles of major elements including Fe, Ni, Cu, Cr, and Ti measured from the steel-interlayer interface to the surface of some of the Ti-rich weld overlays are shown in Figs. 8–10. The concentration of major alloying elements in different layers of the weld overlays is listed in Table 5.

The Fe content in the weld overlay deposits changed from levels near 100 wt-% in the steel substrate to less than 1% through the thickness of the deposited interlayer materials (first layer of the weld overlay). In the case of the Cu-Ti overlay, the Fe level dropped to about 0.35 wt-% within 150 μm from the steel-Cu interface. The Fe content dropped to zero through the first Ti weld layer in most of the overlays. Based on the concentration of Fe in the weld deposit of different interlayers, the weld metal dilution ranges from 2 to 16%. Based on the content of major alloying elements from the interlayer materials in the first Ti layer of the weld overlays, the weld metal dilution ranges from 2 to 20%. Therefore, these results show that the CSC-GMAW process is effective in controlling and minimizing the dilution of the weld metal, which is important in maintaining the corrosion resistance of the Ti-weld deposits.

In the Ni-Ti overlay system, the level of Ni dissolved in the Ti weld metal dropped to 1.3% through the first two Ti layers. In the NiCu-Ti

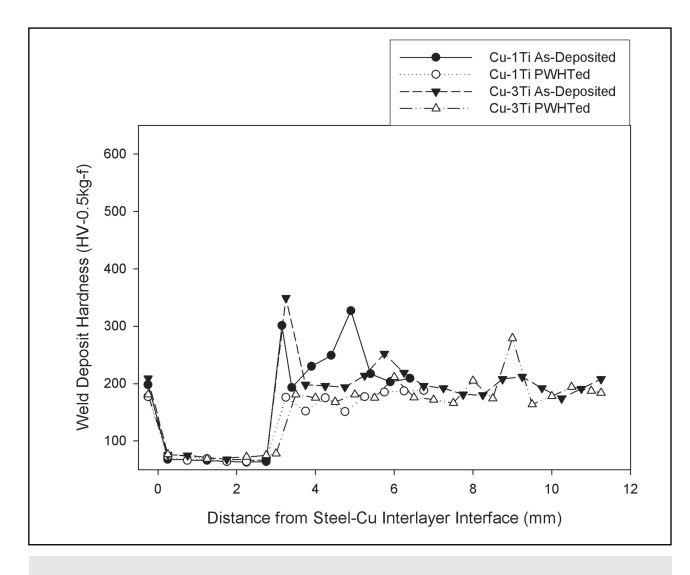


Fig. 12 — Microhardness profile of a Cu-Ti weld metal overlays with one and three Ti layers (1Ti, 3Ti), in the as-welded and PWHT conditions.

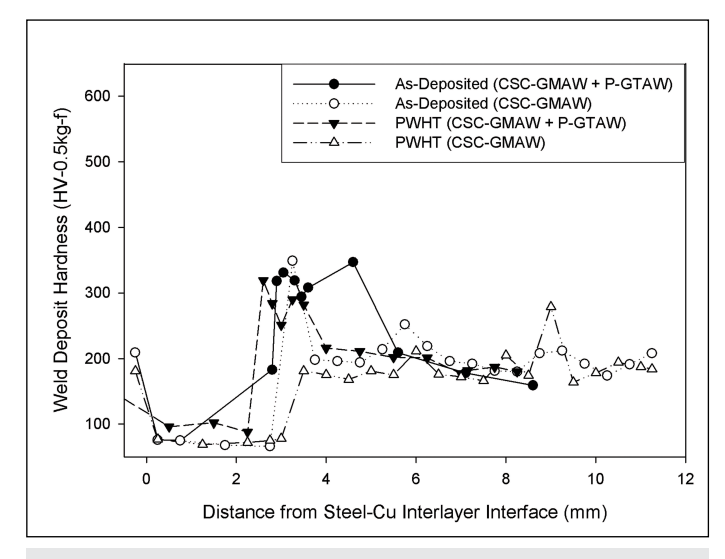


Fig. 13 — Comparison of microhardness profiles of Cu-Ti weld overlay deposited with the CSC-GMAW process and with a combination of CSC-GMAW and GTAW-P processes.

layer, the levels of Ni and Cu dissolved in the Ti weld metal dropped to 3.4 and 1.5%, respectively, through the first two Ti layers, as shown in Fig. 8. In the weld metal made with the NiCr interlayer system, the concentration of both Ni and Cr dissolved in the Ti weld metal dropped to 2.4% through the first two Ti layers. No data were available on the effect of Ni, Cu, or Cr concentration on the corrosion resistance of commercial pure Ti weld metal; however, these results indicate that at least three Ti layers may be required to achieve a commercial pure Ti composition in the surface of the weld overlay for the corrosion resistance needed in some of the Ti-clad applications.

In the Cu-Ti overlay deposited with the CSC-GMAW process, the Cu concentration approximately 100 µm from the Cu/Ti interface was about 1% and remained close to that level through the first Ti weld metal layer, as shown in Fig. 9. This indicates that with the Cu-Ti system deposited with the CSC-GMAW process, only two Ti layers may be needed to achieve the corrosion resistance required for most Ti-clad steel applications. Furthermore, depending on the effect of about 1% Cu on the corrosion resistance of CP Ti weld metals, in some cases one layer of Ti weld metal may be enough to achieve the required corrosion resistance.

In the Cu-Ti overlay deposited with a combination of CSC-GMAW and GTAW-P processes, the concentration

of Cu near to the surface of the second Ti layer is about 0.9%, as shown in Fig. 10. At a distance of 1.5 mm from the surface of the Ti weld metal deposit, the concentration of Cu was 1.1%. Depending on the potential effect of about 1% Cu on the corrosion resistance of Ti, this result indicates that at least three Ti layers may be required to achieve the chemical composition of a CP Ti grade at the surface of the weld deposit exposed to the service medium. The observed microstructure and chemical composition profiles observed in this overlay system may result from a higher degree of intermixing in the weld pool induced by the GTAW-P process compared to the CSC-GMAW process.

Microhardness Profiles: Some of the microhardness profiles obtained from the weld overlays are shown in Figs. 11-13. In general, all weld overlay systems present the highest hardness level at the interlayer-Ti interface and across the first Ti layer. This is in agreement with the results of lightand electron-microscopy characterization of the weld metal deposits that indicated the presence of second phases in those regions of the weld overlays. The maximum hardness in the Ni-Ti, NiCu-Ti, and NiCr-Ti weld overlay systems were 607, 568, and 554 $\mathrm{HV}_{0.5}$, respectively. In the V-Ti and Ti-V overlay systems, the maximum hardness readings obtained at the Fe-V interface were 307 and 409 ${\rm HV}_{0.5}$, respectively. The maximum hardness observed in the Cu-Ti weld overlay ranges from 300 to 350 ${\rm HV}_{0.5}$.

The different weld overlays responded differently to thermal cycles imposed by either welding of additional layers of Ti weld metal or by PWHT. In the Ni-Ti system, a larger softening was caused at the interface and in the first Ti layer by the thermal cycle associated with additional layers of Ti weld metal than by the PWHT. However, as result of the PWHT, the hardness of the weld overlay with three Ti-layers shows some hardening behavior near the interface between the second- and third-Ti layers. In the NiCu-Ti and NiCr-Ti weld overlays, no major softening was observed as a result of the thermal cycles induced either during welding or by PWHT as shown in Fig. 11. The high hardness and softening behavior of these three Ti-rich weld overlay systems make them attractive for wear/erosion resistant applications.

In the Fe-V-Ti system, extremely high hardness was not observed across the weld deposit in spite of the presence of second phases at the Fe-V interface; however, the presence of microcracks at the Fe-V interface may have influenced the results of the hardness readings. In the Ti-V-Fe system, a high hardness peak was observed at the V-Fe interface, which may have resulted from a combination of Fe and Ti at that interface. The high degree of solid solubility between V

Table 5 – Dilution of Major Alloying Elements in Different Layers of the T-Rich Weld Overlays (Based on EPMA Analysis)

Overlay System	Alloying	Alloy Content (wt-%)					
	Elements	Interlayer	1st Ti Layer	2nd Ti Layer	3rd Ti Layer		
Fe-Ni-Ti	Fe	1.6 - 0.8	0.0	0.0	0.0		
	Ni	matrix	19.1 - 10.5	1.3 - 0.0	0.0		
	Ti	3.1 - 3.6	matrix	matrix	matrix		
Fe-NiCu-Ti	Fe	6.5 - 0.8	0.35 - 0.33	0.0	0.0		
	Ni	matrix	16.3 - 13.7	0.4 - 3.4	0.0		
	Cu	matrix	7.5 - 6.2	1.5 - 0.0	0.0		
	Ti	1.9 - 2.5	matrix	matrix	matrix		
Fe-NiCr-Ti	Fe	16.0 - 0.0	0.0	0.0	0.0		
	Ni	matrix	13.7 - 8.1	2.4 - 0.0	0.0		
	Cr	matrix	13.1 - 8.1	2.4 - 0.0	0.0		
	Ti	0.4 -0.8	matrix	matrix	matrix		
Fe-Cu-Ti	Fe	1.3 - 0.0	0.0	0.0	NA		
(CSC-GMAW +	Cu	matrix	13.4 - 2.3	1.1 - 0.9	NA		
GTAW-P)	Ti	0.0	matrix	matrix	NA		
Fe-Cu-Ti	Fe	2.4 - 0.0	0.0	0.0	0.0		
(CSC-GMAW)	Cu	matrix	1.3 - 0.9	0.0	0.0		
	Ti	0.0	matrix	matrix	matrix		

and Ti may have induced a relatively high concentration of Ti in the V weld deposit that could have then been available for reaction with Fe at the V-Fe interface. EPMA analysis was not conducted in weld metal deposits made with either the Fe-V-Ti system or the Ti-V-Fe system to confirm this.

As shown in Fig. 12, the Cu-Ti weld overlay shows the softest deposits, especially in the PWHT condition. This system shows a more pronounced softening behavior due to PWHT than by additional welding thermal cycles. In the Cu-Ti system, as a result of the PWHT, the hardness level through the weld deposit drops to around 200 HV_{0.5}. However, the weld overlay deposited with a combination of CSC-GMAW and GTAW-P processes presented a wider hard region at the Cu-Ti interface and a lower degree of softening induced by the PWHT as shown in Fig. 13. The observed hardness behavior can be explained based on a wider Cu-Ti interface in weld metal deposited with a combination of CSC-GMAW and GTAW-P processes as compared to that deposited with the CSC-GMAW process alone.

Conclusions

• Based on their metallurgical characteristics, compatibility with the Fe-Ti system, and their availability as commercial welding wires, the interlayer materials selected as candidates for Ti-rich weld overlays included commercially pure nickel (CPNi), nickel-copper alloy (NiCu), nickel-chromium alloy (NiCr), CP vanadium (V), and CP copper (Cu).

- The Ni-Ti, NiCu-Ti, and NiCr-Ti weld overlays deposited with the CSC-GMAW process showed a continuous and wide interface between the interlayer material and the first Ti layer. Second phases were observed at the interlayer-Ti interface and in the first Ti layer. In the NiCr-Ti weld overlay, second phases were observed even in the third Ti layer. The first and second Ti layers in these weld overlays presented an acicular- or Widmanstätten- α microstructure that is characteristic in α or α - β Ti alloys.
- The Cu-Ti and V-Ti weld overlays deposited with the CSC-GMAW process and the GTAW-P process, respectively, presented a continuous and well-defined interface between the interlayer material and the first Ti layer. The thickness of the interface ranges from 0 to 250 μm . Second phases were observed at the Cu-Ti interface. The interface between V and Ti was free of second phases. The microstructure of the first Ti layer was similar to those normally found in CP α -Ti alloys.
- The Cu-Ti weld overlay deposited using a combination of CSC-GMAW and GTAW-P processes presented a

continuous and wider interface than that observed in the weld overlay deposited only with the CSC-GMAW process. The thickness of the interface was about 1 mm. The first and second Ti layer presented an acicular- or Widmanstätten- α microstructure.

- The primary second phases identified as potentially present in the Tirich weld overlays include $\mathrm{Ni_3Ti}$, NiTi , $\mathrm{NiTi_2}$, CuNiTi , $\mathrm{CuTi_2}$, $\mathrm{Cr_2Ti}$, $\mathrm{CuTi_2}$, $\mathrm{Cu_3Ti}$, and $\beta\text{-Ti}$.
- The dilution of the interlayer weld metals by the steel base metal ranges from 2 to 16%. The dilution of the first Ti layer in the weld overlays ranges from 2 to 20%. Therefore, the CSC-GMAW process is effective in controlling and minimizing the dilution of the weld metals, which is important in achieving the corrosion resistance of CPTi in the weld overlays with few (one to three) Ti layers.
- In general, the highest hardness in the weld overlays was observed in the interlayer-Ti interface and first Ti layer. The maximum hardness in the Ni-Ti, NiCu-Ti, and NiCr-Ti weld overlays was 607, 568, and 554 HV $_{0.5}$, respectively. Limited degree of softening was induced in these overlays by weld thermal cycles or PWHT. Therefore, these Ti-rich overlay systems could be attractive for wear/erosion resistant applications.
- The maximum hardness observed in the Cu-Ti weld overlay ranged from 300 to 350 HV $_{0.5}$. As a result of the PWHT, the hardness level through the weld deposit dropped to around 200 HV $_{0.5}$. Therefore, this overlay system might be more attractive for mainly corrosion-resistant applications.

Acknowledgments

This publication was prepared based on development work supported by DMC Clad Metal, Materials Technology Institute, and Eastman Chemical as part of a group-sponsored project at EWI.

References

- 1. Banker, J. G. 1996. Titanium-steel explosion clad. *Stainless Steel World*, pp. 65–69 (June).
 - 2. Hardwick, R. 2001. Advances leading

- to the new clads on the future. Stainless Steel World, pp. 149-154.
- 3. Banker, J. G. 1993. Bonded titanium/steel components. U.S. Patent 5,190,831 (March).
- 4. Murayama, J., and Komizo, Y. 1991. Titanium-clad steel and a method for the manufacture thereof. European Patent 0 238 854 B1 (Feb.).
- 5. Hardwick, R. 1993. Method for producing clad metal plate. European Patent 0 535 817 A2 (April).
- 6. Suenaga, H., Ishikawa, M., and Ninakawa, K. 1993. Method for manufacturing titanium clad steel plate. European Patent 0 406 688 B1 (March).
- 7. Kawanami, T., Shirasuna, S., Shirogane, S., and Segawa, A. 1992. An investigation of the characteristic of bonding strength in titanium clad steel. Titanium '92 Science and Technology, Vol. II, Proceedings of a Symposium sponsored by the Titanium Committee on Minerals, Metals & Materials, Structural Metals Division. Held at Seventh World Titanium Conference, San Diego, Calif., edited by F. H. Froes and I. L. Caplan, pp. 1609-1617 (June-July).
- 8. Pin´kovskii, I. V., et al. 1988. Special features of resistance welding VT1-0 titanium to low carbon steel. Welding International No. 3, pp. 241, 242.
- 9. Ramirez, J. E. 2012. Development of joining technology for titanium-clad steel plates. Internal communication at EWI.
- 10. Mitchell, D. R., and Kessler, H. D. 1961. Welding of titanium to steel. Welding Journal 40(12): 546-s to 552-s.

- 11. Feige, N. G. 1979. Method of joining titanium clad steel plates. U.S. Patent 4,142,664 (March).
- 12. Konyukhov, A. V., Sannikov, V. I., Ivanov, B. V., Semenov, V. G., Martem yanova, Z. S., and Rossokhin, B. G. 1982. Welding titanium-clad steel. Avt. Svarka, No. 11, pp. 43-46.
- 13. Semenov, B. G., et al. 1983. Examination of the possibilities of using plasma sprayed refractory carbides as the dividing layer in welding titanium-steel bimetal. Translation No. VR/2905/85, Theoretical Examination Application of Wear Resistant Plasma Coatings in Practice. Sverdlovsk, pp. 27-31.
- 14. Enjyo, T., Ikeuchi, K., Iida, T., Kanai, M., and Arata, Y. 1976. Diffusion welding of Ti-15%Mo-5%Zr alloy to mild steel (0.06%C). Transactions of JWRI 5(1):
- 15. Momono, T., Enjo, T., and Ikeuchi, K. 1990. Effects of carbon content on the diffusion bonding of iron and steel to titanium. ISIJ International 30(11): 978-984.
- 16. Hasui, A., and Kira, Y. 1985. Friction welding of titanium and carbon steel. Transactions of the Japan Welding Society 16(1): 64-69.
- 17. Branko, B. 1992. Composite weldable stud and method for using same. European Patent 0 478 166 A2 (April).
- 18. Zhang, Y. C., Nakagawa, H., and Matsuda, F. 1987. Proposal of new bonding technique "instantaneous liquid phase (ILP) bonding." Transactions of JWRI 16(1): 17-29.
 - 19. Arata, Y., Matsuda, F., and Harada,

- S. 1975. Electron beam welding of carbon steel and titanium sheets using Ag insert metal. Transaction of JWRI 4(2): 71-75.
- 20. Hume-Rothery, W. 1966. Acta Metallurgy 14(1): 17-20.
- 21. Darken, L. S., and Gurry, R. W. 1953. Physical Chemistry of Metals. New York, N.Y.: McGraw Hill, p. 86.
- 22. Marya, M., and Liu, S. 2001. Search for filler metals for welding of ferrous alloys to titanium. Science and Technology of Welding and Joining 6(4): pp. 240-246.
- 23. Miedema, A. R. 1975. Inorganic Chemistry. Dordrech, North-Holland, pp.
- 24. Chelikowski, J. R., and Phillips, J. C. 1978. Phys. Rev. B 17B(6): 2453-2477.
- 25. Huismann, G. 2001. Energy based synergistic MIG control system. IIW Doc.
- 26. Huismann, G. 1999. Introduction of a new MIG process: Advantages and possibilities. IIW Doc. 212-952-99.
- 27. Huismann, G. 2000. Direct Control of the material transfer: The controlled short circuiting (CSC)-MIG process. Proceedings on GMA for the 21st Century, Orlando, Fla., pp. 165-172.
- 28. Huismann, G. 2002. Energy based synergistic pulsed MIG control system. Proceedings of Trends in Welding Research, Pine Mountain, Ga.
- 29. Huismann, G. 2001. Advantages in using the stick out for increasing the burn off rate in gas metal arc welding. 7th International Symposium of Japan Welding Society. Kobe, Japan.

Call for Papers JOM-18

18th International Conference on Joining Materials

Institute for the Joining of Materials in association with IIW Helsingør, Denmark, April 26-29, 2015

Download the brochure detailing topics, expenses, and registration form at:

www.aws.org/wj/JOM-18-CallForPapers.pdf

Review the brochure for conference topics. E-mail a title and short abstract of your paper before Nov. 2, 2014. You will receive author guidelines for preparation of the full paper by Nov. 30. The full paper for publication in the Conference Proceedings must be received by Jan. 15, 2015. E-mail to jom_aws@post10.tele.dk.







